Indirect shared control for cooperative driving between driver and automation in steer-by-wire vehicles

Article (Accepted Version)

Indirect Shared Control for Cooperative Driving between Driver and Automation in Steer-by-Wire Vehicles

Renjie Li, Yanan Li, Shengbo Eben Li, Chaofei Zhang, Etienne Burdet and Bo Cheng

***Abstract*—It is widely acknowledged that drivers should remain in the control loop before automated vehicles completely meet real-world operational conditions. This paper presents an "indirect shared control" framework for steer-by-wire vehicles, which allows the control authority to be continuously shared between the driver and automation through an weighted-input-summation method. A "best-response" driver steering model based on model predictive control (MPC) for indirect shared control is proposed. Unlike any conventional driver model for manual driving, this model assumes that drivers can learn and incorporate the controller strategy into their internal model for predictive path following. The analytic solution to the driver model is provided to enable off-line simulations. A driving-simulator experiment was conducted to demonstrate the advantages of the indirect shared control system in a highway lane-keeping task. The result showed that the proposed indirect shared control method was effective to improve the subjects' lane-keeping performance and reduce steering control effort. The proposed driver steering model was also validated by the experiment data, which produced a smaller prediction error than the conventional MPC driver model.**

***Index Terms*—Shared control, automated vehicles, human-machine interaction, steer-by-wire.**

I. Introduction

In recent years, several ambitious automated-driving projects, *e.g.*, Google (now Waymo) self-driving car and Tesla Autopilot, have seen rapid progress towards commercialization. Automated vehicles are considered as an effective approach to relieve human drivers of tedious driving tasks through advanced sensing and navigation technologies, yet various issues need to be addressed before their ultimate deployment. These issues include technical requirements, safety problems, ethical dilemmas, and subsequent harsh government regulations. In addition, previous studies have shown that imperfect vehicle automation may give rise to severe human factor problems such as loss of situation awareness and over-reliance [1], [2], which would increase the risk of accidents when the automated driving system malfunctions. These problems are usually believed to be caused by drivers being kept out of the operating loop when the automation is in complete charge of vehicle control.

This research is supported by National Key R&D Program of China with 2017YFB0102603, NSF China with U1664263 and UK EPSRC grant EP/T006951/1. All correspondence should be sent to S. E. Li (e-mail: lisb04@gmail.com).

R. Li, S. E. Li, C. Zhang and B. Cheng are with the State Key Lab of Automotive Safety and Energy, Tsinghua University, Beijing, China 100084 (e-mail: lirenaxe@gmail.com; lisb04@gmail.com; zhangcfthu10@163.com; chengbo@tsinghua.edu.cn).

Y. Li and E. Burdet are with the Department of Bioengineering, Imperial College London, UK SW7 2AZ (e-mail: hit.li.yn@gmail.com; e.burdet@imperial.ac.uk). Y. Li is also with the Department of Engineering and Design, University of Sussex, Brighton, UK BN1 9RH.

To cope with the above issues, it is widely acknowledged that human drivers with relatively superior capabilities to deal with complicated situations should be kept in the control loop before fully automated driving systems become available. For instance, in some semi-autonomous driving schemes [3]–[6], the human driver assumes control most of the time, whereas the assistant controller only intervenes if it anticipates imminent dangers. Therefore, the benefit of automation is limited to merely short durations. By contrast, shared control schemes aim to provide continuous support to human drivers, wherein the assistant controller persistently takes part in vehicle control. It was reported that the shared control technology can reduce drivers' workload and improve their performance in a broad range of driving tasks [7].

A basic form of shared control is known as the haptic shared control, which is realized by an active haptic feedback to assist drivers in common driving scenarios [8]. Despite a few early studies on haptic-feedback gas pedals for longitudinal control assistance [9], haptic shared control has been mostly employed in lateral control tasks, *i.e.*, lane keeping [10], [11], curve negotiation [12], and lane change [13], wherein the driver and automation perform steering cooperatively through physical interaction. The beneficial effects of haptic shared control are surveyed in [7], and the methods to design the controllers include look-ahead feedback [14], optimal preview control [10], fuzzy control [11], [15], model predictive control (MPC) [16], and game theory [17]. The mechanism of haptic shared control has been studied in other fields such as human-robot interaction [18], [19] where it is referred to as "motor interaction" or "joint motor action" [20]. The implementation of haptic shared control is rooted in the fact that conventional mechanical steering systems can only support physical steering assistance, usually by means of a torque motor connected with the steering column.

In contrast to mechanical steering systems, steer-by-wire technology allows the mechanical decoupling of the steering wheel from the road wheels. With steer-by-wire, it is possible for an intermediate controller to modulate the driver's steering command by a low-level steering actuator. For this reason, steer-by-wire technology lays the basis for another type of shared control, where the controller is able to complement the driver's steering without a direct physical interaction. This shared control paradigm is referred to as "indirect shared control" in our previous works [21], [22], and also called "input-mixing shared control" in [14]. Indirect shared control offers better flexibility for controller design, as the driver's steering input can be transformed before being delivered to the front wheels. Accordingly, the driver's control authority depends on how we design the intermediate controller to assimilate their steering command. Previous works relying

on similar steering input transformation techniques mainly focused on active intervention in emergency situations [4], [5], [23], whereas its use in routine steering tasks has been somehow overlooked. In [24], the authors provided a dynamic steering-ratio adjustment method for steer-by-wire vehicles, which can be deemed as a specific realization of indirect shared control. Compared with haptic shared control, indirect shared control has the potential to further minimize the driving effort because the driver is not obligated to provide full steering. Moreover, the assistant controller in indirect shared control does not interfere with the driver's steering operations directly. This property can possibly reduce the driver's control effort to compete with the controller.

Important problems that need to be resolved to establish indirect shared control include: 1) how to design an intermediate assistant controller such that it can respect the driver input while exploiting its own strength; 2) how to model drivers' adaptive behavior in presence of a given assistant controller such that the indirect shared control system can be evaluated through fast off-line simulations. Some studies on haptic shared control such as [10], [11] included a driver model in controller design and simulation, but did not consider the driver adaptation which has however been observed in [14]. In fact, numerous studies have documented the adaptation inherent to human sensorimotor control, which has been modeled through the formation of an internal inverse or forward model [25]. This puts forward an intuitive conjecture that the driver adaptation in indirect shared control can be interpreted as the integration of the assistant controller into their internal model.

The primary contributions of this paper are two fold: 1) an indirect shared control framework is presented for lane-keeping assistance of steer-by-wire vehicles, in which the assistant controller adopts a weighted-summation method to blend the driver's commanded input with its own interest. The designed system is provided with explicit and tunable driver-automation control authorities, which is easy for practical implementations; 2) a driver steering model for the proposed framework is established based on an MPC formulation, which interprets the driver's motor adaptation as an update of the internal model. More specifically, it relies on the assumption that the driver is able to identify and incorporate the controller's strategy into her/his internal model and use it to optimize the steering behavior for path following. We call this model the "best-response" driver steering model in this paper, motivated by another study which observed that humans would exhibit such an adapt-and-optimize behavior in collaboration with robot arms [26].

The rest of this paper is organized as follows. Section II describes the framework of indirect shared control and compares it with haptic shared control. Section III designs the indirect shared controller based on a weighted-input-summation strategy with an unconstrained MPC lateral control algorithm. Section IV formulates the driver's steering model that considers human motor adaptation, and derives its analytic solution for fast computing. Section V validates the proposed indirect shared control system and the associated driver steering model by a driving-simulator experiment, and Section VI concludes the paper.

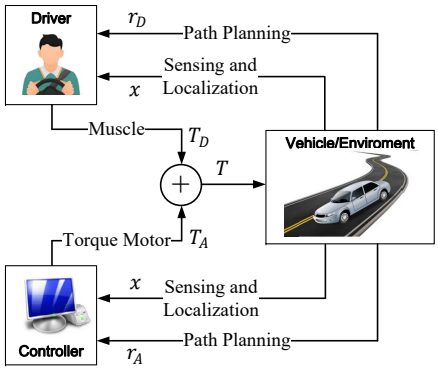

(a) Haptic shared control

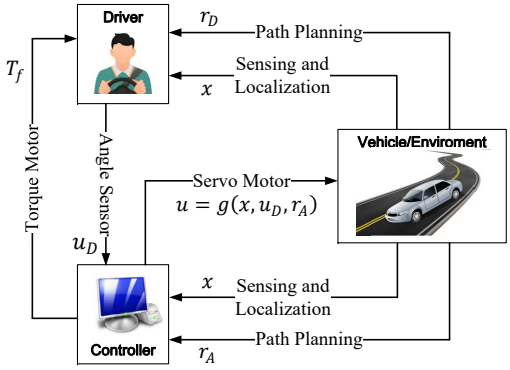

(b) Indirect shared control

Fig. 1: Block diagrams of two shared control frameworks.

II. System Description

The systematic frameworks of haptic and indirect shared control are compared in Fig. 1. In both schemes, the driver and assistant controller continuously receive a desired reference path (denoted by r_D and r_A) from an online path planner, and the vehicle state x through sensing and localization abilities. In haptic shared control, the driver and controller simultaneously apply a control torque (denoted by T_D and T_A) on the steering wheel, and the resultant torque $T = T_D + T_A$ forms the final control input. The primary goal for haptic shared controller design is an appropriate mapping from the current vehicle state x and reference path r_A to the assistant torque T_A. As for indirect shared control, the steering wheel angle u_D is commanded by the driver but observed by an intermediate controller. The driver input u_D does not directly influence the vehicle motion, but is transformed by the controller according to a predesignated function $u = g(x, u_D, r_A)$ before being sent to the low-level steering system. Indirect shared control can be easily implemented on steer-by-wire vehicles because there is no mechanical linkage between the steering wheel and the road wheels. A torque feedback T_f can be provided to enhance driver steering feel, which is however beyond the scope of this study.

In indirect shared control, the driver and controller share the control authority and guide the vehicle in a coopera-

tive fashion. The design of the transformation strategy $u = g(x, u_D, r_A)$ defines how the driver's input and the controller's objective are balanced. In a sense, the driver's control authority depends on how largely u relies on u_D. Here are two extreme cases: if the final input u is independent of the driver input u_D, *i.e.*, $u = g(x, r_A)$, the vehicle becomes fully autonomous because the driver is disengaged from vehicle control; on the other hand, if u completely complies with u_D, *i.e.*, $u = u_D$, indirect shared control actually degrades to manual driving. The indirect shared control scheme guarantees that the driver is actively involved in the control loop because s/he is obligated to convey control input throughout driving. Meanwhile, the driver's steering effort is partly relieved by the intermediate controller, because full and accurate steering operations are no longer required.

III. Indirect Shared Controller Design

A. Input Transformation Strategy

The input transformation strategy $u = g(x, u_D, r_A)$ is crucial for indirect shared control. Shia *et al.* [4] suggested a simple angle overlay $u = u_D + u_A$, where u_A is a corrective steering wheel input calculated by a threat-assessment algorithm. Anderson *et al.* [3] used a weighted-summation method $u = (1 - \lambda)\, u_D + \lambda\, u_A$, where u_A comes from an online MPC lateral control algorithm and the weight λ also depends on the current threat. The assistant controller in these studies plays a role of safety guard and follows the principle of minimum intervention, which means u_A would remain zero at most of the time. To make drivers benefit from the assistant controller's continuous support, we hereby propose a more generic weighted-summation law as the input transformation strategy:

$$u(k) = \lambda_D u_D(k) + \lambda_A u_A(k), \quad \lambda_D, \lambda_A \geq 0\,, \tag{1}$$

where u_A is the controller's desired input calculated from a lateral control algorithm, and λ_D, λ_A are the authority weights assigned to the driver input and the controller's desired input, respectively. The advantage of this method is that the control authorities of the driver and controller are explicitly parametrized as the corresponding weights λ_D and λ_A. Thus, we can change the authority allocation by simply tuning their values. The setting of λ_D and λ_A is not trivial. $\lambda_D + \lambda_A = 1$ is often assumed to avoid conflict and motion instability, as well as to simplify the control authority management using only one parameter. In our previous work [21], we have discussed how to dynamically allocate the control authorities according to the driver intention. In this study, we seek to investigate the effect of indirect shared control under different authority allocations, and hence λ_D and λ_A would remain unchanged. In practical implementations, the drivers would have the freedom to choose from different assistance levels (corresponding to different control authority settings) according to their preference.

There are various lateral control algorithms, among which MPC has been proved to be particularly suitable for vehicle path following [27], [28]. Therefore, we also choose MPC as the control algorithm to calculate the desired input u_A, where an appropriate vehicle model is needed first.

B. Vehicle Model

The vehicle model used is the dynamical bicycle model with respect to the lane centerline [29], as shown in Fig. 2, where CG denotes the vehicle center of mass, D the nearest point along the lane centerline to CG, a the distance from CG to the front axle, b the distance from CG to the rear axle, e_y the lateral displacement error, e_ψ the heading angle error, ρ the lane centerline curvature at D, δ the steering angle, V the longitudinal speed. If the following assumptions are satisfied: 1) the steering angle δ is small which implies small tire sideslip angles, such that the tires work in a linear region, 2) the vehicle heading direction is around the lane centerline, *i.e.*, e_ψ is small, and 3) the longitudinal speed V is (nearly) constant, the bicycle model in continuous-time form can be described by a linear time-invariant equation as

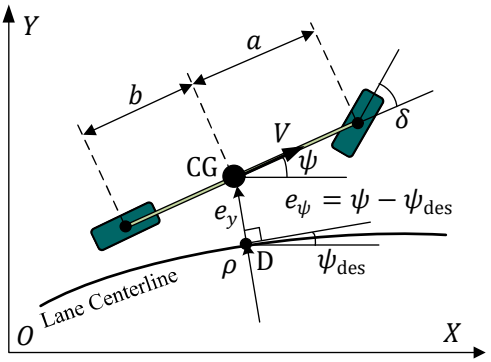

Fig. 2: Dynamic bicycle model in path coordinates.

$$\begin{aligned} \dot{x}_t &= A_c x_t + B_c u_t + E_c \rho_t \\ z_t &= C_c x_t \end{aligned} \tag{2}$$

where the state $x := \begin{bmatrix} \dot{e}_y & \dot{e}_\psi & e_y & e_\psi \end{bmatrix}^{\mathrm{T}}$, the measurement $z := \begin{bmatrix} e_y & e_\psi \end{bmatrix}^{\mathrm{T}}$ and the associated measurement matrix $C_c = \begin{bmatrix} 0 & 0 & 1 & 1 \end{bmatrix}^{\mathrm{T}}$, the model input $u := \delta_s$ is the steering wheel angle which is usually proportional to δ by a constant steering ratio i_s, *i.e.*, $\delta_s = i_s \delta$. A_c, B_c and E_c are constant matrices related to the vehicle's intrinsic properties and the constant longitudinal speed V, calculated by

$$A_c = \begin{bmatrix} \frac{-2(C_f + C_r)}{mV} & \frac{-2(aC_f - bC_r)}{mV} & 0 & \frac{2(C_f + C_r)}{m} \\ \frac{-2(aC_f - bC_r)}{I_z V} & \frac{-2(a^2 C_f + b^2 C_r)}{I_z V} & 0 & \frac{2(aC_f - bC_r)}{I_z} \\ 1 & 0 & 0 & 0 \\ 0 & 1 & 0 & 0 \end{bmatrix}$$

$$E_c = \begin{bmatrix} \frac{2(aC_f - bC_r)}{m} - V^2 \\ -\frac{2(a^2 C_f + b^2 C_r)}{I_z} \\ 0 \\ 0 \end{bmatrix}, \; B_c = \begin{bmatrix} \frac{2C_f}{i_s m} & \frac{2aC_f}{i_s I_z} & 0 & 0 \end{bmatrix}^{\mathrm{T}}$$

where C_f is the front cornering stiffness, C_r the rear cornering stiffness, m the vehicle mass, I_z the polar moment of inertia.

Given a control sampling time T_s, the continuous-time vehicle model (2) can be discretized into a discrete-time form as

$$\begin{aligned} x_{k+1} &= A\,x_k + Bu_k + E\rho_k \\ z_k &= Cx_k \end{aligned} \tag{3}$$

where k denotes discrete time index, A, B, E and C are discrete-time state-space matrices converted from A_c, B_c, E_c and C_c, respectively.

C. MPC Lateral Control Algorithm

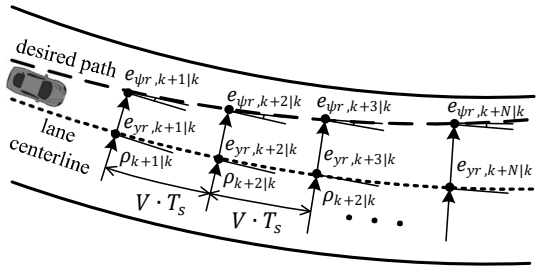

Fig. 3: MPC lateral control.

The basic idea of the MPC lateral control algorithm is illustrated in Fig. 3. At each time step k, the controller previews the desired reference path r_A and samples it at an interval of $V \cdot T_s$ up to a predictive horizon N. The sampled lateral displacement errors $\{e_{yr,k+i|k}\}_{i=1,\cdots,N}$ and associated heading angle errors $\{e_{\psi r,k+i|k}\}_{i=1,\cdots,N}$ constitute the controller's desired trajectory. In addition, it is assumed that the current vehicle state x_k and the previewed road curvatures $\{\rho_{k+i|k}\}_{i=0,\cdots,N-1}$ are observable through the on-board sensors. Then, the controller utilizes the vehicle model (3) as the model predictor and optimizes an input sequence $U_{A,k} := \begin{bmatrix} u_{A,k|k} & \cdots & u_{A,k+N-1|k} \end{bmatrix}^{\mathrm{T}}$ subject to a predefined cost function. The first element of the optimal input sequence is taken as the current control input $u_{A,k}$. Sometimes the decision variables in $U_{A,k}$ are restricted to the first N_c (called "control horizon", $0 < N_c \leq N$) elements to reduce the scale of the optimization problem, but here we assume $N_c = N$ for simplicity. The MPC lateral control algorithm is mathematically formulated as the following:

$$\min_{U_{A,k}} \Big(\sum_{i=1}^{N} \big\| z_{k+i|k} - z_{Ar,k+i|k} \big\|_{Q_A}^2 + \sum_{i=0}^{N-1} \big\| u_{A,k+i|k} \big\|_{R_A}^2 \Big) \tag{4a}$$

$$\text{s.t. } x_{k+i+1|k} = Ax_{k+i|k} + Bu_{A,k+i|k} + E\rho_{k+i|k}, \quad i = 0, \cdots, N-1 \tag{4b}$$

$$z_{k+i|k} = Cx_{k+i|k}, \qquad i = 1, \cdots, N \tag{4c}$$

$$x_{k|k} = x_k \tag{4d}$$

where $z_{Ar} := \begin{bmatrix} e_{yr} & e_{\psi r} \end{bmatrix}^{\mathrm{T}}$ represents the reference path vector, Q_A and R_A are constant positive definite weighting matrices of appropriate dimensions. A convention is to let R_A be unity and Q_A be a diagonal matrix. The quadratic cost (4a) penalizes the accumulative path-tracking error and input magnitude over the predictive horizon. The model predictor (4b) is exactly the dynamic vehicle model (3). In other words, the controller does not consider the driver when calculating its desired input. The unconstrained MPC problem (4) has a standard least-squares solution [30]. We intentionally omit the derivation here but give the analytic solution directly, and interested readers could see Section IV-B and [30] for reference. Define the following vector notations

$$Z_k := \begin{bmatrix} z_{k+1|k} \\ z_{k+2|k} \\ \vdots \\ z_{k+N|k} \end{bmatrix}, Z_{Ar,k} := \begin{bmatrix} z_{Ar,k+1|k} \\ z_{Ar,k+2|k} \\ \vdots \\ z_{Ar,k+N|k} \end{bmatrix}, P_k := \begin{bmatrix} \rho_{k|k} \\ \rho_{k+1|k} \\ \vdots \\ \rho_{k+N-1|k} \end{bmatrix}$$

and matrix notations

$$\Phi := \begin{bmatrix} CA \\ CA^2 \\ \vdots \\ CA^N \end{bmatrix}, \Theta := \begin{bmatrix} CB & 0 & \cdots & 0 \\ CAB & CB & \cdots & 0 \\ \vdots & \vdots & \ddots & \vdots \\ CA^{N-1}B & CA^{N-2}B & \cdots & CB \end{bmatrix}$$

$$\Omega := \begin{bmatrix} CE & 0 & \cdots & 0 \\ CAE & CE & \cdots & 0 \\ \vdots & \vdots & \ddots & \vdots \\ CA^{N-1}E & CA^{N-2}E & \cdots & CE \end{bmatrix}$$

$$\mathcal{Q}_A\,(\mathcal{R}_A) := \begin{bmatrix} Q_A\,(R_A) & & & \\ & Q_A\,(R_A) & & \\ & & \ddots & \\ & & & Q_A\,(R_A) \end{bmatrix} \Bigg\} N$$

The analytic solution to the MPC lateral control algorithm is given as

$$U_{A,k} = \mathcal{K}_A \big(Z_{Ar,k} - \Phi x_k - \Omega P_k \big) \tag{5}$$

and

$$u_{A,k} = e_1^{\mathrm{T}} U_{A,k} = e_1^{\mathrm{T}} \mathcal{K}_A \big(Z_{Ar,k} - \Phi x_k - \Omega P_k \big) \tag{6}$$

where $e_1^{\mathrm{T}} := \overbrace{\begin{bmatrix} 1 & 0 & \cdots & 0 \end{bmatrix}}^{N}$, $\mathcal{K}_A := \begin{bmatrix} \sqrt{\mathcal{Q}_A}\Theta \\ \sqrt{\mathcal{R}_A} \end{bmatrix}^{\dagger} \begin{bmatrix} \sqrt{\mathcal{Q}_A} \\ 0 \end{bmatrix}$ ('†' denotes pseudo-inverse) is a constant gain matrix. By defining a generalized path-tracking error vector as

$$\varepsilon_{A,k} := Z_{Ar,k} - \Phi x_k - \Omega P_k \tag{7}$$

The solution (6) can be simplified as

$$u_{A,k} = e_1^{\mathrm{T}} \mathcal{K}_A \varepsilon_{A,k} \tag{8}$$

IV. Best-Response Driver Steering Model for Indirect Shared Control

A. Model Formulation

Some previous studies found that human drivers can formulate an internal model of the vehicle dynamics after motor learning, and use it as the model predictor for predictive steering control (illustrated in Fig. 4(a)), and proposed MPC-based methods to model driver steering behavior in path following [31], [32]. Compared with manual driving, the essence of indirect shared control can be regarded as transforming the vehicle's input-output characteristic (from the driver's perspective) by inserting an intermediate controller (see Fig. 4(b)). Thus, it is assumed that drivers would still perform predictive

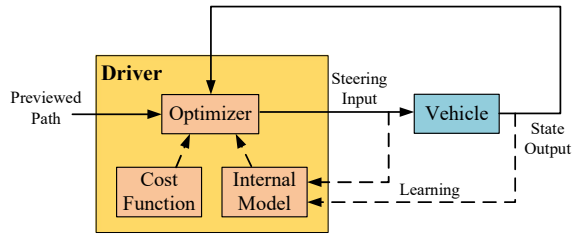

(a) Manual control

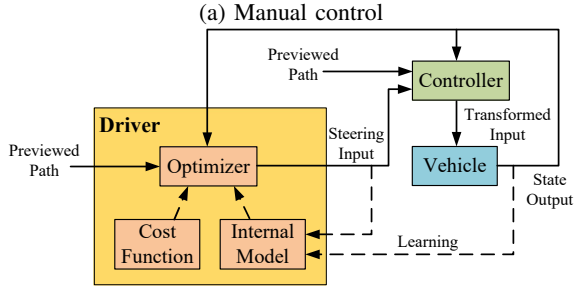

(b) Indirect shared control

Fig. 4: MPC-based driver steering model in two control frameworks.

steering in indirect shared control, except that the internal model becomes the modified vehicle dynamics adapted by the driver. Based on this assumption, we present an MPC-based driver steering model for indirect shared control, formulated as (we assume the driver's predictive horizons are identical to the controller's for simplifying derivation)

$$\min_{U_{D,k}} \left(\sum_{i=1}^{N} \left\| z_{k+i|k} - z_{Dr,k+i|k} \right\|_{Q_D}^2 + \sum_{i=0}^{N-1} \left\| u_{D,k+i|k} \right\|_{R_D}^2 \right) \tag{9a}$$

$$\text{s.t. } x_{k+i+1|k} = Ax_{k+i|k} + \lambda_D B u_{D,k+i|k} + \lambda_A B \hat{u}_{A,k+i|k} + E\rho_{k+i|k}, \quad i = 0, \cdots, N-1 \tag{9b}$$

$$z_{k+i|k} = Cx_{k+i|k}, \quad i = 1, \cdots, N \tag{9c}$$

$$x_{k|k} = x_k \tag{9d}$$

where the notations are similar to those defined in Section III-C. The above driver model formulation is similar to the conventional MPC (4) except that the model predictor (9b) includes not only the original vehicle dynamics but also the weighted-summation law (1) and the driver's prediction of the controller's desired input $\hat{u}_A$ up to the predictive horizon. This major difference comes from our modeling assumption that the driver is able to incorporate the controller's input transformation strategy into her/his internal model after motor adaptation. The above model can be interpreted as the driver would optimize her/his steering behavior in response to her/his prediction of the controller's assistant behavior.

B. Analytic Solution

One way to use the best-response driver steering model (9) is to treat it as a quadratic program and solve it numerically, where the predicted inputs would be passed into the solver as online parameters. However, we want an analytic solution to the model to improve computational efficiency and simulation accuracy. By treating the predicted input $\hat{u}_A$ and the path curvature ρ as external disturbances, it is possible to follow the least-squares approach in [30] to obtain its analytic solution.

Again, we add the following notations which are similar to those defined in Section III-C:

$$Z_{Dr,k} := \begin{bmatrix} z_{Dr,k+1|k} \\ z_{Dr,k+2|k} \\ \vdots \\ z_{Dr,k+N|k} \end{bmatrix}, \quad \hat{U}_{A,k} := \begin{bmatrix} \hat{u}_{A,k|k} \\ \hat{u}_{A,k+1|k} \\ \vdots \\ \hat{u}_{A,k+N-1|k} \end{bmatrix}$$

$$\mathcal{Q}_D(\mathcal{R}_D) := \begin{bmatrix} Q_D(R_D) & & & \\ & Q_D(R_D) & & \\ & & \ddots & \\ & & & Q_D(R_D) \end{bmatrix} \Bigg\} N$$

Iterating (9b) from $i = 0$ to $N-1$, (9c) from $i = 1$ to N and using the defined notations, we have

$$Z_k = \Phi x_k + \lambda_D \Theta U_{D,k} + \lambda_A \Theta \hat{U}_{A,k} + \Omega P_k \tag{10}$$

On the other hand, the optimization problem (9a) can be converted to the following form by using the notations:

$$\min_{U_{D,k}} \left(\|Z_k - Z_{Dr,k}\|_{\mathcal{Q}_D}^2 + \|U_{D,k}\|_{\mathcal{R}_D}^2 \right) \tag{11}$$

Define the generalized error vector for the driver as

$$\varepsilon_{D,k} := Z_{Dr,k} - \Phi x_k - \Omega P_k \tag{12}$$

and the optimization problem (11) can be further converted to

$$\min_{U_{D,k}} \left\| \begin{matrix} \sqrt{\mathcal{Q}_D}\left(\lambda_D \Theta U_{D,k} + \lambda_A \Theta \hat{U}_{A,k} - \varepsilon_{D,k}\right) \\ \sqrt{\mathcal{R}_D} U_{D,k} \end{matrix} \right\|^2 \tag{13}$$

which is equivalent to solving

$$\min_{U_{D,k}} \left\| \begin{bmatrix} \lambda_D \sqrt{\mathcal{Q}_D}\Theta \\ \sqrt{\mathcal{R}_D} \end{bmatrix} U_{D,k} - \begin{bmatrix} \sqrt{\mathcal{Q}_D} \\ 0 \end{bmatrix} \left(\varepsilon_{D,k} - \lambda_A \Theta \hat{U}_{A,k} \right) \right\|^2 \tag{14}$$

The solution to the least-squares problem above is

$$\begin{aligned} U_{D,k} &= \begin{bmatrix} \lambda_D \sqrt{\mathcal{Q}_D}\Theta \\ \sqrt{\mathcal{R}_D} \end{bmatrix}^{\dagger} \begin{bmatrix} \sqrt{\mathcal{Q}_D} \\ 0 \end{bmatrix} \left(\varepsilon_{D,k} - \lambda_A \Theta \hat{U}_{A,k} \right) \\ &= \mathcal{K}_D \left(\varepsilon_{D,k} - \lambda_A \Theta \hat{U}_{A,k} \right) \end{aligned} \tag{15}$$

where the gain matrix $\mathcal{K}_D := \begin{bmatrix} \lambda_D \sqrt{\mathcal{Q}_D}\Theta \\ \sqrt{\mathcal{R}_D} \end{bmatrix}^{\dagger} \begin{bmatrix} \sqrt{\mathcal{Q}_D} \\ 0 \end{bmatrix}$. Finally, the driver's steering control at time k is modeled by

$$u_{D,k} = e_1^{\mathrm{T}} \mathcal{K}_D \left(\varepsilon_{D,k} - \lambda_A \Theta \hat{U}_{A,k} \right) \tag{16}$$

Comparing the above best-response driver steering model expression (16) with the conventional MPC model, *i.e.*, the controller's desired input algorithm (8) with parameters replaced by the drivers, we find their main differences lie in 1) the gain matrix $\mathcal{K}_D$ depends on not only the driver's weighting matrix Q_D but also her/his control authority λ_D, and 2) the error term includes the driver's prediction of controller's predicted input sequence $\hat{U}_A$ by the factor of its authority λ_A, in addition to the generalized error vector ε_D.

We can briefly examine the driver model (16) by checking two boundary cases, *i.e.*, manual driving ($\lambda_D = 1$, $\lambda_A = 0$) and fully autonomous driving ($\lambda_D = 0$, $\lambda_A = 1$):

1) In the manual driving case ($\lambda_D = 1$ and $\lambda_A = 0$), the gain matrix $\mathcal{K}_D := \begin{bmatrix} \sqrt{\mathcal{Q}_D}\Theta \\ \sqrt{\mathcal{R}_D} \end{bmatrix}^{\dagger} \begin{bmatrix} \sqrt{\mathcal{Q}_D} \\ 0 \end{bmatrix}$, and the error term is solely $\varepsilon_{D,k}$. The driver model (16) becomes the solution to a basic unconstrained MPC lateral control problem, degrading to the conventional MPC model.

2) In the autonomous driving case ($\lambda_D = 0$ and $\lambda_A = 1$), the gain matrix $\mathcal{K}_D = \begin{bmatrix} 0 \\ \sqrt{\mathcal{R}_D} \end{bmatrix}^{\dagger} \begin{bmatrix} \sqrt{\mathcal{Q}_D} \\ 0 \end{bmatrix} = \mathbf{0}$, which yields a trivial solution $u_{D,k} = 0$. This means that if the driver realizes that s/he has no control authority, s/he would not operate the steering wheel. This is in line with our intuition.

In order to use the best-response driver model to simulate indirect shared control systems, it should be specified how to set up the prediction sequence $\hat{U}_A$ aside from other ordinary parameters such as Q_D and N. It is suggested that if the controller adopts an MPC-based method to calculate the desired input, the controller's open-loop control sequence U_A at each time step can be passed to the driver model to serve as the driver's prediction $\hat{U}_A$; if the controller employs non-MPC methods, zeroth-order prediction or first-order prediction can be used for convenience.

For the controller designed in this paper which uses MPC lateral control as the desired input algorithm, the corresponding driver steering model expression is immediately obtained by substituting (5) into (16) as $\hat{U}_A$:

$$u_{D,k} = e_1^{\mathrm{T}} \mathcal{K}_D \left(\varepsilon_{D,k} - \lambda_A \Theta \mathcal{K}_A \varepsilon_{A,k} \right) \tag{17}$$

V. Experimental Validation

A. Apparatus and Measurement

The experiment was conducted in a driving simulator in Tsinghua University, as shown in Fig. 5. The cockpit is transformed from a BMW sedan, and the moving base supports six degree-of-freedom motion to imitate real driving. The road scene is projected onto five surrounding screens (three in the front and two in the rear), providing 200 deg field of view in the front and 55 deg in the rear. The sound of engine, wind, *etc.*, are created by an audio simulation unit. The vehicle dynamics is simulated by the CarSim D-class sedan, which outputs the vehicle state at 60 Hz. An external control interface is available for real-time control, which can receive the driver's steering wheel angle as well as the vehicle state and output a steering input overlay at 60 Hz. The vehicle state (including the vehicle position and yaw angle at the global coordinates) and the driver's steering wheel angle were collected as driving data. The overall experiment setup is illustrated in Fig. 6.

Fig. 5: Driving simulator in the Tsinghua University (left: outside; right: inside).

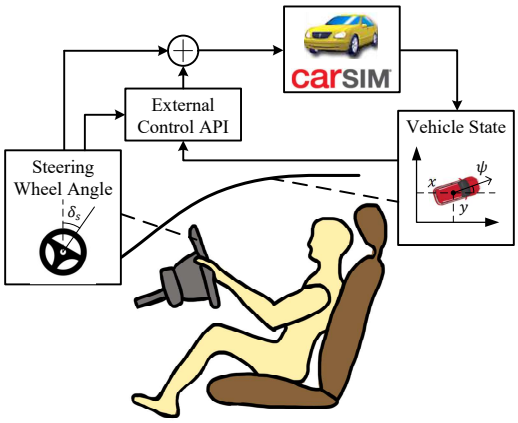

Fig. 6: Experiment setup.

B. Settings and Procedure

The experiment scenario was a three-lane highway. The test track consists of five fixed-radius curves and every two curves are connected by a straight road, as shown in Fig. 7. The total length of the test track is about 17 km. The maximum curve radius (curve ③) is 3,993 meters and the minimum (curve ④) is 307 meters. The vehicle speed was fixed at 90 km/h (25 m/s) by the program. The MPC controller parameters are listed in Table I. The vehicle parameters were taken from the CarSim data sheet. The predictive horizon N_p and weighting matrix Q_A were properly tuned such that the controller could keep lane well in the autonomous mode. The state-space matrices were discretized by the Matlab function *c2d*.

Six subjects possessing driver licenses (five males and one female) were recruited to participate the experiment. The subjects were asked to keep the vehicle along the middle lane center and not to move their hands off the steering wheel until the test trial was over. The experiment was conducted in three conditions: manual ($\lambda_D = 1, \lambda_A = 0$), low assistance (LA, $\lambda_D = 0.8, \lambda_A = 0.2$), and high assistance (HA, $\lambda_D = 0.3, \lambda_A = 0.7$) with one test trial per condition. The lane centerline was designated as the controller's reference path, and the controller's parameters (including vehicle model parameters, predictive horizon and weighting matrices) were properly tuned to exhibit satisfactory lane-keeping performance. The subjects were trained to get used to the simulator

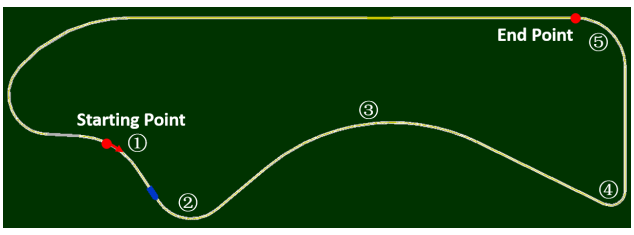

Fig. 7: Test track.

TABLE I: Controller parameters.

Parameter	Value
C_f	97,088 [N/rad]
C_r	59,317 [N/rad]
a	1.1 [m]
b	1.776 [m]
m	1,134 [kg]
I_z	1,750 [kg·m^2]
i_s	16.9
V	25 [m/s]
T_s	1/60 [s]
N	90
Q_A	$diag$(0.1, 1)

and the controller's assistance before the real test of each condition. The subjects were allowed to take a five-minute break after each test to prevent drowsiness. The driving data from the simulator was collected for further analysis after the experiment.

C. System Evaluation

The indirect shared control system was evaluated in two aspects: lane-keeping performance and the driver's steering control effort. In terms of lane-keeping performance, we examined the vehicle's tracking error from the lane centerline. For steering control effort, we focused on the intensity of driver's steering activity (reflected by steering wheel angles). To investigate the influence of shared control level, we computed the following evaluation metrics from the collected driving data for each trial.

• *Tracking error metrics*: the vehicle lateral displacement error e_y and heading angle error e_ψ with respect to the lane centerline were first calculated from the driving data. Then, we extracted the RMS (root mean square) value of the lateral displacement error $\mathrm{rms}(e_y)$ and yaw error $\mathrm{rms}(e_\psi)$, which indicate the vehicle lane-keeping performance.

• *Steering effort metric*: we evaluate the subjects' steering control effort by estimating their average power exerted on the steering wheel. Considering that 1) the self-aligning torque on the steering wheel was approximately proportional to the steering wheel angle and 2) since we did not measure the subjects' steering torque directly in the experiment, it was assumed equal to the self-aligning torque when the steering wheel was moved away from the neutral position and zero otherwise, we used the following metric $\bar{P}_{\mathrm{str}}$ to estimate the average human steering power:

$$\begin{aligned} \Delta W_i &= \begin{cases} u_{D,i}\cdot\Delta u_{D,i}, & u_{D,i}\cdot\Delta u_{D,i} > 0 \\ 0, & u_{D,i}\cdot\Delta u_{D,i} \le 0 \end{cases} \\ \bar{P}_{\mathrm{str}} &= \frac{\sum_{i=2}^{n}\Delta W_i}{t_n - t_1} \end{aligned} \tag{18}$$

where $\Delta u_{D,i} := u_{D,i} - u_{D,i-1}$, t_i is the time for the i-th data point, n is the length of the valid data in a test trial. Note that $\bar{P}_{\mathrm{str}}$ is roughly proportional to the real average steering power, and its unit is deg^2/s.

Figure 8 depicts the driving data metrics for each subject in different modes. On top of that, the averages of the metrics are also added to better demonstrate their general trends over the assistance level. First, let us investigate the tracking error metrics. It is observed from Fig. 8 that the lane-keeping performance for most subjects (except subject E who performed worst in LA mode) improved with a higher assistance level, as the tracking error metrics $\mathrm{rms}(e_y)$ and $\mathrm{rms}(e_\psi)$ dropped evidently when the controller's authority was increased. In comparison, results of the steering effort metric $\bar{P}_{\mathrm{str}}$ show more variability. Figure 8 shows that for some subjects (C and F), their average steering effort was reduced with increasing assistance. But for other subjects (A, B and D), their steering effort slightly increased when the assistance level increased. For subject E, the energy consumption in HA was even higher than the manual mode. These results demonstrated that the designed indirect shared control system (either in LA or HA) was effective to relieve the steering control effort for most subjects, while the individual difference is interpreted as due to the subjects' personal driving characteristics. For subjects whose reference path was close to the lane centerline (and hence close to the controller's reference path), their steering rate and magnitude both went down in HA because they shared a mutual goal with the controller. Conversely, for subjects who tended to cut curves, they would apply a large steering angle in HA to compensate for the controller's lane-centering effort. Therefore, although their steering rate in HA was also lower, the average energy consumption might be even higher. This interesting result indicates a future direction to improve the present shared control system: if the driver and controller's intended reference paths could be coordinated, the driver's steering effort in shared control would be further reduced.

D. Driver Model Validation

In this section, we validate the proposed best-response driver steering model by estimating the model parameters using the experiment data and evaluating the prediction error, *i.e.*, the residual. Prior to that, an explicit parametrized driver model is needed. We expand the driver model (17) to

$$\begin{aligned} u_{D,k} = e_1^{\mathrm{T}} &\begin{bmatrix} \lambda_D\sqrt{\mathcal{Q}_D}\Theta \\ \sqrt{\mathcal{R}_D} \end{bmatrix}^{\dagger} \begin{bmatrix} \sqrt{\mathcal{Q}_D} \\ 0 \end{bmatrix} \left(Z_{Dr,k} - \Phi x_k - \Omega P_k \right. \\ &\left. - \lambda_A\Theta \begin{bmatrix} \sqrt{\mathcal{Q}_A}\Theta \\ \sqrt{\mathcal{R}_A} \end{bmatrix}^{\dagger} \begin{bmatrix} \sqrt{\mathcal{Q}_A} \\ 0 \end{bmatrix} Z_{Ar,k} - \Phi x_k - \Omega P_k \right) \end{aligned} \tag{19}$$

Note that the matrices Θ, Φ, Ω, $\mathcal{R}_D$, $\mathcal{Q}_A$, $\mathcal{R}_A$ are all constant, and the controller's reference path is fixed at the lane centerline hence $Z_{Ar} = \mathbf{0}$, we can rewrite the expanded driver steering model (19) as a concise function

$$u_{D,k} = h(x_k, P_k, \lambda_D, \lambda_A, Q_D, Z_{Dr,k}) \tag{20}$$

From the identification perspective, in (20) the driver steering input u_D, vehicle state x and previewed road curvature

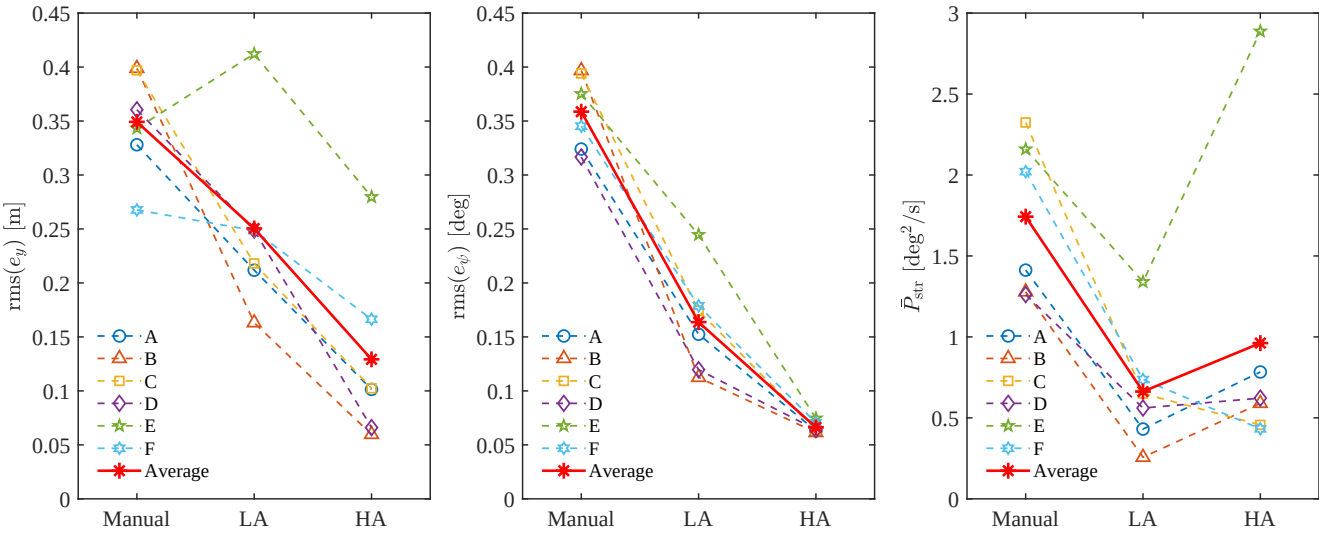

Fig. 8: Driving data metrics in different modes.

vector P are observable signals from experiment data, the control authorities λ_D and λ_A are known parameters per test trial, and the remaining variables Q_D is an unknown parameter and $Z_{D,r}$ is an unknown signal. The task is to identify Q_D in presence of the unknown driver reference path signal $Z_{D,r}$ from the observed data and known parameters.

If we consider the driver model as a lateral controller, this is a typical closed-loop identification problem [33]. The biggest challenge here is the unknown signal $Z_{D,r}$ which makes Q_D almost unidentifiable. To resolve this problem, we assume that the subjects' desired reference path on a fixed-radius curve has a constant deviation from the lane centerline. This assumption makes $Z_{Dr,k} \equiv Z_{Dr}$ also a parameter in the model expression, which can be thus identified along with Q_D. We adopted the least-squares method to estimate Q_D and Z_{Dr} (denote the estimates as $\hat{Q}_D$ and $\hat{Z}_{Dr}$):

$$\begin{aligned} err(Q_D, Z_{Dr}) &= \tilde{u}_{D,k} - h\big(\tilde{x}_k, \tilde{P}_k, \lambda_D, \lambda_A, Q_D, Z_{Dr}\big) \\ \langle \hat{Q}_D, \hat{Z}_{Dr} \rangle &= \underset{Q_D, Z_D}{\arg\min} \sum_{i=1}^{n} \|err(Q_D, Z_{Dr})\|^2 \end{aligned} \tag{21}$$

where $\tilde{u}_D$, $\tilde{x}$ and $\tilde{P}$ are from the experiment measurement, and λ_D, λ_A are exactly the allocated control authorities in the corresponding experiment condition.

Eq. (21) is a nonlinear least-squares problem. We used the *lsqnonline* function in Matlab to solve it, which is based on the trust-region-reflective algorithm. Considering that the subjects' steering input on straight roads are so small that the identification process cannot be excited adequately, we only kept the curvy-road driving data for the parameter identification. Furthermore, it is likely that drivers' reference path deviation may differ with the road curvature, so the identification was performed per curve for each subject. All the related data were smoothed by a fourth-oder low-pass Butterworth filter before being fed into the identification function.

First, we compare the original steering angle profile measured in the experiment with that predicted by the identified driver steering model for a rough and qualitative validation. The result of subject D is selected as an example, as shown in Fig. 9(a) and Fig. 9(b). In general, the driver model can reproduce the experiment data in terms of average steering magnitude but fails to capture the microscopic features especially when the assistance level is low.

To validate the proposed best-response driver steering model quantitatively, the RMS value of the model prediction error for each subject is depicted in Fig. 9(c), in which the result for the manual mode is also added for comparison. We can tell from Fig. 9(c) that:

1) the average prediction error of the best-response driver steering model is below 1 deg (except for subject E the average prediction error for which locates from 1.1 deg to 1.7 deg), either in LA or HA mode;

2) for most subjects, the model prediction error is smaller for LA and HA than for manual driving, which indicates that the proposed driver steering model is particularly suitable for indirect shared control.

In an attempt to further demonstrate the advantage of the proposed best-response driver steering model, we re-performed the identification on the same experiment data set using the conventional MPC driver model. The prediction error of the conventional model is given in Fig. 9(d). It should be noted that the best-response driver model would degrade to the conventional MPC model for manual driving, thus the prediction errors in manual mode are the same for the two models. By comparing Fig. 9(c) and Fig. 9(d), we can easily find that the prediction error of the proposed model is generally smaller, which proves that the best-response driver steering model better describes human behavior in interaction with the controller and is thus more suitable to be adopted in simulations.

VI. Conclusion and Future Directions

This paper investigated an indirect driver-automation shared control framework for steer-by-wire vehicles. A weighted-summation method was used to balance the interests of the driver and assistant controller, where their control authorities

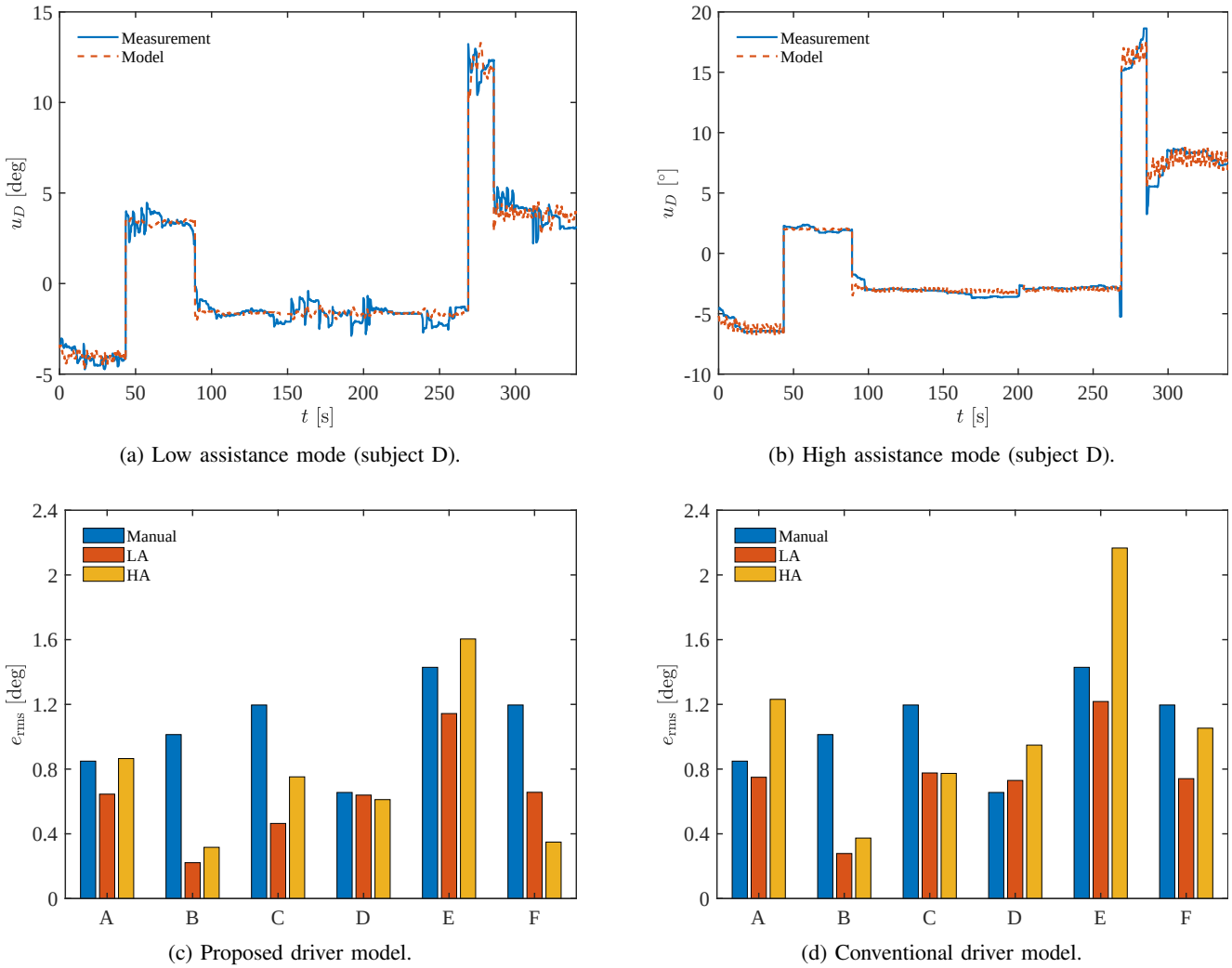

(a) Low assistance mode (subject D).

(b) High assistance mode (subject D).

(c) Proposed driver model.

(d) Conventional driver model.

Fig. 9: Validation of the driver model.

were defined as the weights assigned to their inputs. A best-response driver steering model was proposed to reproduce drivers' steering behavior in indirect shared control, and the analytic solution was given to improve computational efficiency and accuracy for simulation implementation.

The indirect shared control system was validated by an driving-simulator experiment in a highway lane-keeping scenario. The driving data analysis showed that the designed system significantly improved the drivers' lane-keeping performance and reduced their steering control effort, demonstrated by an evident reduction of path-tracking error and driver steering power. The best-response driver steering model was also verified by the experiment data. After identification, the average prediction error of the model is smaller than that of the conventional MPC driver steering model.

For future research, it would be interesting to find out how to infer the driver's intended path in shared control and thus improve the controller design to further enhance the driver's comfort. Moreover, how to arbitrate between the driver and controller if they disagree with each other in different scenarios would also be a challenging topic.

References

[1] N. Merat, A. H. Jamson, F. C. Lai, and O. Carsten, "Highly automated driving, secondary task performance, and driver state," *Human Factors: The Journal of the Human Factors and Ergonomics Society*, vol. 54, no. 5, pp. 762–771, 2012.

[2] M. Saffarian, J. De Winter, and R. Happee, "Automated driving: human-factors issues and design solutions," in *Proceedings of the Human Factors and Ergonomics Society Annual Meeting*, vol. 56, pp. 2296–2300, Sage Publications, 2012.

[3] S. J. Anderson, S. B. Karumanchi, K. Iagnemma, and J. M. Walker, "The intelligent copilot: A constraint-based approach to shared-adaptive control of ground vehicles," *IEEE Intelligent Transportation Systems Magazine*, vol. 5, no. 2, pp. 45–54, 2013.

[4] V. A. Shia, Y. Gao, R. Vasudevan, K. D. Campbell, T. Lin, F. Borrelli, and R. Bajcsy, "Semiautonomous vehicular control using driver modeling," *IEEE Transactions on Intelligent Transportation Systems*, vol. 15, no. 6, pp. 2696–2709, 2014.

[5] S. M. Erlien, S. Fujita, and J. C. Gerdes, "Shared steering control using safe envelopes for obstacle avoidance and vehicle stability," *IEEE Transactions on Intelligent Transportation Systems*, vol. 17, no. 2, pp. 441–451, 2016.

[6] F. Altché, X. Qian, and A. de La Fortelle, "An algorithm for supervised driving of cooperative semi-autonomous vehicles," *IEEE Transactions on Intelligent Transportation Systems*, vol. 18, no. 12, pp. 3527–3539, 2017.

[7] S. M. Petermeijer, D. A. Abbink, M. Mulder, and J. C. de Winter, "The effect of haptic support systems on driver performance: A literature survey," *IEEE Transactions on Haptics*, vol. 8, no. 4, pp. 467–479, 2015.

[8] D. A. Abbink, M. Mulder, and E. R. Boer, "Haptic shared control: smoothly shifting control authority?," *Cognition, Technology & Work*, vol. 14, no. 1, pp. 19–28, 2012.
[9] D. A. Abbink, E. R. Boer, and M. Mulder, "Motivation for continuous haptic gas pedal feedback to support car following," in *Intelligent Vehicles Symposium, 2008 IEEE*, pp. 283–290, IEEE, 2008.
[10] L. Saleh, P. Chevrel, F. Claveau, J.-F. Lafay, and F. Mars, "Shared steering control between a driver and an automation: Stability in the presence of driver behavior uncertainty," *IEEE Transactions on Intelligent Transportation Systems*, vol. 14, no. 2, pp. 974–983, 2013.
[11] A.-T. Nguyen, C. Sentouh, and J.-C. Popieul, "Driver-automation cooperative approach for shared steering control under multiple system constraints: Design and experiments," *IEEE Transactions on Industrial Electronics*, vol. 64, no. 5, pp. 3819–3830, 2017.
[12] Z. Wang, R. Zheng, T. Kaizuka, and K. Nakano, "The effect of haptic guidance on driver steering performance during curve negotiation with limited visual feedback," in *Intelligent Vehicles Symposium (IV), 2017 IEEE*, pp. 600–605, IEEE, 2017.
[13] K. K. Tsoi, M. Mulder, and D. A. Abbink, "Balancing safety and support: Changing lanes with a haptic lane-keeping support system," in *Systems Man and Cybernetics (SMC), 2010 IEEE International Conference on*, pp. 1236–1243, IEEE, 2010.
[14] D. A. Abbink and M. Mulder, "Neuromuscular analysis as a guideline in designing shared control," in *Advances in haptics*, InTech, 2010.
[15] A. T. Nguyen, C. Sentouh, and J.-C. Popieul, "Sensor reduction for driver-automation shared steering control via an adaptive authority allocation strategy," *IEEE/ASME Transactions on Mechatronics*, 2017.
[16] Z. Ercan, A. Carvalho, M. Gokasan, and F. Borrelli, "Modeling, identification, and predictive control of a driver steering assistance system," *IEEE Transactions on Human-Machine Systems*, vol. 47, no. 5, pp. 700–710, 2017.
[17] M. Flad, L. Fröhlich, and S. Hohmann, "Cooperative shared control driver assistance systems based on motion primitives and differential games," *IEEE Transactions on Human-Machine Systems*, 2017.
[18] Y. Li, K. P. Tee, W. L. Chan, R. Yan, Y. Chua, and D. K. Limbu, "Continuous role adaptation for human–robot shared control," *IEEE Transactions on Robotics*, vol. 31, no. 3, pp. 672–681, 2015.
[19] Y. Li, K. P. Tee, R. Yan, R. Yan, W. L. Chan, and Y. Wu, "A framework of human–robot coordination based on game theory and policy iteration," *IEEE Transactions on Robotics*, vol. 32, no. 6, pp. 1408–1418, 2016.
[20] N. Jarrassé, V. Sanguineti, and E. Burdet, "Slaves no longer: review on role assignment for human–robot joint motor action," *Adaptive Behavior*, vol. 22, no. 1, pp. 70–82, 2014.
[21] R. Li, Y. Li, S. E. Li, E. Burdet, and B. Cheng, "Driver-automation indirect shared control of highly automated vehicles with intention-aware authority transition," in *Intelligent Vehicles Symposium (IV), 2017 IEEE*, pp. 26–32, IEEE, 2017.
[22] R. Li, S. Li, H. Gao, K. Li, B. Cheng, and D. Li, "Effects of human adaptation and trust on shared control for driver-automation cooperative driving," tech. rep., SAE Technical Paper, 2017.
[23] X. Na and D. J. Cole, "Application of open-loop stackelberg equilibrium to modeling a driver's interaction with vehicle active steering control in obstacle avoidance," *IEEE Transactions on Human-Machine Systems*, 2017.
[24] W. Wang, J. Xi, C. Liu, and X. Li, "Human-centered feed-forward control of a vehicle steering system based on a driver's path-following characteristics," *IEEE transactions on intelligent transportation systems*, vol. 18, no. 6, pp. 1440–1453, 2016.
[25] E. Burdet, D. W. Franklin, and T. E. Milner, *Human robotics: neuromechanics and motor control*. MIT Press, 2013.
[26] S. Nikolaidis, S. Nath, A. D. Procaccia, and S. Srinivasa, "Game-theoretic modeling of human adaptation in human-robot collaboration," in *2017 12th ACM/IEEE International Conference on Human-Robot Interaction (HRI*, pp. 323–331, IEEE, 2017.
[27] G. V. Raffo, G. K. Gomes, J. E. Normey-Rico, C. R. Kelber, and L. B. Becker, "A predictive controller for autonomous vehicle path tracking," *IEEE transactions on intelligent transportation systems*, vol. 10, no. 1, pp. 92–102, 2009.
[28] X. Du, K. K. K. Htet, and K. K. Tan, "Development of a genetic-algorithm-based nonlinear model predictive control scheme on velocity and steering of autonomous vehicles," *IEEE Transactions on Industrial Electronics*, vol. 63, no. 11, pp. 6970–6977, 2016.
[29] R. Rajamani, *Vehicle dynamics and control*. Springer Science & Business Media, 2011.
[30] J. M. Maciejowski, *Predictive control: with constraints*. Pearson education, 2002.
[31] D. Cole, A. Pick, and A. Odhams, "Predictive and linear quadratic methods for potential application to modelling driver steering control," *Vehicle System Dynamics*, vol. 44, no. 3, pp. 259–284, 2006.
[32] T. Qu, H. Chen, D. Cao, H. Guo, and B. Gao, "Switching-based stochastic model predictive control approach for modeling driver steering skill," *IEEE Transactions on Intelligent Transportation Systems*, vol. 16, no. 1, pp. 365–375, 2015.
[33] L. Ljung, "System identification," in *Signal analysis and prediction*, pp. 163–173, Springer, 1998.

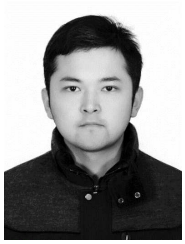

Renjie Li received the BEng degree and PhD degree from the Department of Automotive Engineering of Tsinghua University, China, in 2013 and 2018, respectively, where he is currently working as a post-doctoral researcher. He was also a visiting PhD student at the Department of Bioengineering, Imperial College, London, UK. His research interests include human-machine interaction and vehicle dynamical control.

Yanan Li (S'10-M'14) received the BEng and MEng degrees from the Harbin Institute of Technology, China, in 2006 and 2008, respectively, and the PhD degree from the National University of Singapore, in 2013. Currently he is a Lecturer in Control Engineering with the Department of Engineering and Design, University of Sussex, UK. From 2015 to 2017, he has been a Research Associate with the Department of Bioengineering, Imperial College London, UK. From 2013 to 2015, he has been a Research Scientist with the Institute for Infocomm Research (I2R), Agency for Science, Technology and Research (A*STAR), Singapore. His general research interests include human-robot interaction, assistive robotics, human motor control and control theory and applications.

Shengbo Eben Li received the M.S. and Ph.D. degrees from Tsinghua University in 2006 and 2009. Before joining Tsinghua University, he has worked at Stanford University, University of Michigan, and UC Berkeley. He is now leading Intelligent Driving Lab (iDLab) at Tsinghua University. His active research interests include intelligent vehicles and driver assistance, reinforcement learning and optimal control, distributed control and estimation, etc. He is the author of over 100 peer-reviewed journal/conference papers. Dr. Li was the recipient of the National Award for Technological Invention of China (2013), Excellent Young Scholar of NSF China (2016), Young Professorship of Changjiang Scholar Program (2016), Tsinghua University Excellent Professorship Award (2017), National Award for Progress in Science and Technology of China (2018), Distinguished Young Scholar of Beijing NSF (2018), etc. He also serves as Board of Governor of IEEE ITS Society, AEs of IEEE ITSM, IEEE Trans ITS, IJCT, and Vehicle, etc.

Chaofei Zhang received the BEng degree in vehicle engineering from Tsinghua University, Beijing, China, in 2010, where he is currently working toward the Ph.D. degree in mechanical engineering. He is currently with the State Key Laboratory of Automotive Safety and Energy, the Department of Automotive Engineering, Tsinghua University. He was also a visiting Ph.D. student in the Harvard Medical School, Harvard University, Boston, USA. His research interests include driver musculoskeletal modeling and autonomous vehicle control.

Etienne Burdet (S'92-M'96) received the MS degree in mathematics, the MS degree in physics, and the PhD degree in robotics, all from ETH-Zurich, Switzerland. He is Professor and Chair in Human Robotics at Imperial College London, and his main research interest is in human-machine interaction. He uses an integrative approach of neuroscience and robotics to investigate human sensorimotor control, and to design efficient assistive devices and training systems for neuro-rehabilitation, which are tested in clinical trials.

Bo Cheng received his bachelor and master degree from Tsinghua University (1985/1988), and Ph.D. from Tokyo University (1998). He is now the professor of Tsinghua University, Dean of Tsinghua University-Suzhou Automotive Research Institute, Deputy Director of State Key Lab of Automotive Safety and Energy. His active research interests include autonomous vehicles, driver assistance systems, active safety, vehicular ergonomics, etc. He is the author of more than 70 journal/conference papers, and the co-inventor of more than 20 patents. He also works as Chairman of Academic Board of SAE-Beijing, Member of Council of Chinese Ergonomics Society, Committee Member of National 863 Plan, Member of Academic Committee of China Transportation Technology Project, etc.